

1
2
3
4
5
6
7
8
9
10
11
12
13
14
15
16
17
18
19
20
21

Photosynthesis-irradiance responses in the Ross Sea, Antarctica: a meta-analysis

W.O. Smith, Jr. and K. Donaldson

Virginia Institute of Marine Science, College of William & Mary, Gloucester Pt., VA 23062, USA

Correspondence to: W.O. Smith, Jr. (wos@vims.edu)

Submitted to *Biogeosciences*

Running Head: Ross Sea photosynthesis

April 21, 2015

22 Abstract

23 A meta-analysis of photosynthesis/irradiance measurements was completed using data from
24 the Ross Sea, Antarctica using a total of 417 independent measurements. P_m^B , the maximum,
25 chlorophyll-specific, irradiance-saturated rate of photosynthesis, averaged $1.1 \pm 0.06 \mu\text{g C} (\mu\text{g}$
26 $\text{chl})^{-1} \text{h}^{-1}$. Light-limited, chlorophyll-specific photosynthetic rates (α^B) averaged 0.030 ± 0.023
27 $\mu\text{g C} (\mu\text{g chl})^{-1} \text{h}^{-1} (\mu\text{mol quanta m}^{-2} \text{s}^{-1})^{-1}$. Significant variations in P_m^B and α^B were found as a
28 function of season, with spring maximum photosynthetic rates being 60% greater than those in
29 summer. Similarly, α values were 48% greater in spring. There was no detectable effect of
30 sampling location on the photosynthetic parameters, and temperature and macronutrient (NO_3)
31 concentrations also did not have an influence. However, irradiance and carbon dioxide
32 concentrations, when altered under controlled conditions, exerted significant influences on
33 photosynthetic parameters. Specifically, reduced irradiance resulted in significantly decreased
34 P_m^B and increased α^B values, and increased CO_2 concentrations resulted in significantly
35 increased P_m^B and α^B values. Comparison of photosynthetic parameters derived at stations
36 where iron concentrations were above and below 0.1 nM indicated that reduced iron levels were
37 associated with significantly increased P_m^B values, confirming the importance of iron within the
38 photosynthetic process. No significant difference was detected between stations dominated by
39 diatoms and those dominated by the haptophyte *Phaeocystis antarctica*. The meta-analysis
40 confirms the photosynthetic rates predicted from global analyses that are based solely on
41 temperature and irradiance availability, but suggests that for more accurate predictions of
42 productivity in polar systems, a more detailed model that includes temporal effects of
43 photosynthetic parameters will be required.

44 1. Introduction

45 The relationship of phytoplankton photosynthesis to irradiance is fundamental not only to our
46 understanding of marine productivity, but also in predicting the response of marine systems to
47 climate change and other anthropogenic alterations (Brown and Arrigo, 2012; Huot et al., 2013).
48 This is especially true in high-latitude systems, where modifications in ice cover will bring
49 dramatic changes in available irradiance and hence productivity (e.g., Montes-Hugo et al., 2008;
50 Arrigo et al., 2013; Smith et al., 2014b), as well as changes in air-sea interactions and food-web
51 dynamics (Smith et al., 2014a). Photosynthesis-irradiance (P-E) relationships are also essential
52 components of estimating productivity from satellite remote sensing data, as productivity is
53 generally modeled as a function of integrated chlorophyll concentrations, available irradiance,
54 and the P-E response as a function of temperature (Behrenfeld and Falkowski, 1997; Platt et al.,
55 2007). The temperature-photosynthesis relationship is generally assumed to be constant below
56 0°C (Behrenfeld and Falkowski, 1997), despite the fact that substantial oceanographic variability
57 is known in other variables that influence photosynthesis in these low temperature seas.

58 P-E responses are generally described by a relatively simple equation that parameterizes the
59 response as a function of irradiance: P_s^B , the biomass-specific rate of photosynthesis at
60 saturating irradiances in the absence of photoinhibition, α^B , the irradiance-limited, biomass-
61 specific linear portion of the hyperbolic response, and β^B , the portion of the curve where
62 photosynthesis decreases at high irradiances (photoinhibition) (Platt et al., 1980a). P_m^B is the
63 biomass-specific, realized rate of photosynthesis at saturating irradiances. A parameter
64 describing the irradiance at which saturation is initiated, E_k , is derived from the ratio of P_m^B and
65 α^B . Chlorophyll *a* concentrations are generally used as an index of biomass. Estimates of
66 photoinhibition are often difficult to obtain and are thought to represent a non-steady state

67 condition (Marra et al., 1985), and measurements often do not result in statistically significant
68 estimates of β^B (van Hilst and Smith, 2002; Huot et al., 2013); hence β^B is often assumed to be
69 zero.

70 P-E responses from the Southern Ocean have been assessed from a number of regions (e.g.,
71 West Antarctic Peninsula: Brightman and Smith, 1989; Moline et al., 1998; Scotia Sea: Tilzer et
72 al., 1986; Ross Sea: van Hilst and Smith, 2002; Robinson et al., 2003; Smyth et al., 2012), but
73 unlike for the Arctic Ocean (Platt et al., 1980b; Huot et al., 2013), no synthesis of photosynthetic
74 responses or their environmental controls is available. Different investigators also have used
75 slightly different methods, making a comparison more difficult; furthermore, because regions in
76 the Southern Ocean change rapidly, it is challenging to interpret the results of changing P-E
77 responses in the context of spatial and temporal variability of oceanographic conditions. In
78 general, phytoplankton in the Southern Ocean exhibit low maximum photosynthetic rates
79 (between 1 and 2 $\mu\text{g C } (\mu\text{g chl})^{-1} \text{ h}^{-1}$), and E_k values reflect the in situ irradiance environment
80 from which the phytoplankton were sampled. That is, when phytoplankton are sampled from
81 within a deeply mixed surface layer or from under the ice, E_k values are low, reflecting an
82 acclimation to reduced available irradiance. Conversely, E_k values generally increase when
83 phytoplankton are sampled from stratified, ice-free environments in summer that are
84 characterized by higher mean irradiance values.

85 The Ross Sea is among the best studied areas in the Antarctic, and a great deal is known
86 about its oceanography, productivity, temporal and spatial variability, and food web dynamics
87 (Smith et al., 2012, 2014b). Despite a broad understanding of the system's characteristics, a full
88 synthesis of the area's photosynthesis-irradiance relationships is lacking. It is known that the
89 colonial haptophyte *Phaeocystis antarctica* typically blooms in austral spring and reaches high

90 abundance (Tremblay and Smith, 2007; Smith et al., 2014a), and disappears rapidly from the
91 water column after reaching its seasonal maximum (Smith et al., 2011a). Laboratory and field
92 investigations have shown that *P. antarctica* is well adapted to grow at low and variable
93 irradiances characteristic of deeply mixed surface layers and under variable ice cover
94 (Kroupenske et al., 2009; Arrigo et al., 2010). In contrast, diatoms often bloom after *P.*
95 *antarctica* is reduced in biomass, but the magnitude of the diatom growth is highly variable
96 among years (Peloquin and Smith, 2007). Diatoms are in general capable of growth at higher
97 photon flux densities, characteristic of stratified, summer conditions and close proximity to
98 melting sea ice (Arrigo et al., 2010). The general distributions of both functional groups suggest
99 that the photosynthetic capacity of each is different and reflects the in situ habitat that each is
100 found. Despite this, van Hilst and Smith (2002) and Robinson et al. (2003) were unable to show
101 a statistically significant difference between the P-E responses of samples dominated by one
102 functional group or the other. This suggests that the distribution of functional groups may be
103 strongly influenced by factors other than just photosynthesis, despite photophysiological abilities
104 and acclimations to different environments.

105 This study synthesizes the results from a large number of photosynthesis-irradiance
106 measurements conducted at various times and locations in the Ross Sea. Given the generally
107 predictable pattern of phytoplankton growth in the area (*Phaeocystis antarctica* blooms upon the
108 removal of ice in relatively deep water columns, and drive the biomass maximum in late spring,
109 and are followed by diatom growth; Smith et al., 2014b), we assessed the photosynthetic
110 responses as a function of season. We also compared the various environmental controls (e.g.,
111 temperature, nitrate, and iron) on irradiance-saturated photosynthetic rates, as well as their
112 relationship to assemblage composition.

113

114 **2. Methods**

115 *2.1. Analytical Procedures*

116 Samples were collected during a number of cruises, most of which concentrated their
117 sampling in the southern Ross Sea (Fig. 1). The first was IVARS (Interannual Variations in the
118 Ross Sea; Smith et al., 2011a,b), which collected samples during short cruises twice each year,
119 with the first cruise sampling ice-free periods in late December and the second sampling the end
120 of summer (early February). The second project was CORSACS (Controls on Ross Sea Algal
121 Community Structure), which had two cruises. The first cruise began in late December, 2005
122 and the second was in November-December, 2006 (Sedwick et al., 2011; Smith et al., 2013). P-
123 E results from CORSACS involved controlled, experimental manipulations of irradiance,
124 dissolved iron and CO₂ concentrations and used trace-metal clean procedures (Feng et al., 2010;
125 Rose et al., 2010). The final project was PRISM (Processes Regulating Iron Supply at the
126 Mesoscale), which sampled in January-February, 2012 (Smith and Jones, 2014; McGillicuddy et
127 al., in press). Figure 1 shows the locations of the stations analyzed for photosynthesis/irradiance
128 relationships. Published measurements from other investigations are also included in the meta-
129 analysis (e.g., van Hilst and Smith, 2002; Robinson et al., 2003; Saggiomo et al., 2004; Hiscock,
130 2004; Smyth et al., 2012).

131 Photosynthesis-irradiance (P-E) relationships of phytoplankton were determined by assessing
132 uptake of ¹⁴C-bicarbonate in short incubations (Lewis and Smith, 1983). The largest difference
133 among the different published reports was sample filtration; samples that were not filtered thus
134 included any short-term DOC release (Table 1). Robinson et al. (2003) concluded that filtration
135 of samples dominated by colonial *Phaeocystis antarctica* resulted in an underestimate of
136 photosynthetic rates, but comparison within IVARS and CORSACS did not identify this

137 systematic bias (Smith, unpublished). Samples were generally collected from one or two depths
 138 (generally that of the 50 and 1% isolumes) at each station (50% depths were generally from 1-4
 139 m, and 1% depths from 15-50 m), to which ca. 100-150 $\mu\text{Ci NaH}^{14}\text{CO}_3$ were added. Incubations
 140 were conducted at a constant temperature from the depth of sampling (determined by the CTD
 141 cast and maintained by a circulating water bath). Samples were placed in glass scintillation vials
 142 in a photosynthetron that provided a wide range of irradiances, but ultraviolet radiation was
 143 excluded by the incubation design. Photosynthetically available radiation was modified from the
 144 maximum value by neutral density screening at irradiances ca. 70% of the full irradiance, and by
 145 a combination of neutral and blue screening at lower irradiances (Laws et al., 1990). Darkened
 146 vials served as controls. Irradiance was measured for each sample; the total number of
 147 irradiances used ranged from 16 to 32. Incubations lasted approximately 2 h. All samples were
 148 counted on liquid scintillation counters, and total available inorganic ^{14}C -bicarbonate was
 149 assessed by counting aliquots of the original solution directly in scintillation fluor. While details
 150 of the methods of each study varied somewhat, we were unable to detect a significant difference
 151 between filtered and unfiltered results, and concluded that the methods did not introduce a
 152 significant source of error to obscure the overall patterns.

153 All data were fitted to the rectilinear hyperbolic model of Platt et al. (1980b):

$$154 \quad P^B = P_m^B \left[1 - e^{-\alpha^B E / P_m^B} \right] \quad (\text{Eq. 1})$$

155 where P^B = the rate of photosynthesis normalized to chlorophyll a [$\text{mg C (mg chl } a)^{-1} \text{ h}^{-1}$], P_m^B =
 156 the maximum realized, irradiance-saturated rate of photosynthesis, α^B = the initial, light-limited,
 157 linear photosynthetic rate normalized to chlorophyll [$\text{mg C (mg chl } a)^{-1} \text{ h}^{-1} (\mu\text{mol quanta m}^{-2}$

158 s^{-1}], and E = irradiance ($\mu\text{mol quanta m}^{-2} \text{s}^{-1}$). All responses were fit to a 2-parameter
159 exponential increase to maxima in SigmaPlot 12.3, which provided estimates of P_m^B and α^B and
160 their significance, as determined by a t-test. Some of the published analyses included β^B , the
161 photoinhibition parameter, but for consistency these were omitted in this meta-analysis, since β^B
162 appears to represent a non-equilibrium condition and in our samples was not consistently evident
163 (Denman and Marra, 1986; MacIntyre et al., 2002). Photoinhibitory data from stations where
164 photoinhibition occurred were not removed, as the impact on photosynthetic parameters was
165 generally minor. The derived parameter E_k (the irradiance at which photosynthesis becomes
166 saturated) is calculated by:

$$167 \quad E_k = P_m^B / \alpha^B \quad (\text{Eq. 2})$$

168 E_k provides a measure by which the acclimation to irradiance can be compared. If the
169 observations did not result in a significant determination of both α^B and P_m^B ($p < 0.05$), then the
170 entire sample was omitted from the meta-analysis.

171 Chlorophyll a concentrations were analyzed by fluorometry (JGOFS, 1996) on independent
172 samples collected from the same depth. Nutrient (NO_3 , NO_2 , PO_4 , Si(OH)_4 , NH_4) analyses were
173 performed at sea on a Lachat QuickChem Autanalyzer using standard automated techniques, or
174 on frozen samples after return to the laboratory. Mixed layer depths were determined from
175 density profiles determined from CTD casts using a change in density of 0.01 kg m^{-3} from a
176 stable surface value (Thomson and Fine, 2003; Smith et al., 2013). Seawater samples for
177 dissolved iron analysis were collected in custom-modified 5-L Teflon-lined, external-closure
178 Niskin-X samplers (General Oceanics Inc.) or 10-L teflon-lined GO-FLO samplers, all of which
179 were deployed on a non-metal line (Sedwick et al., 2011). Filtered samples were acidified to pH

180 1.7 with ultrapure hydrochloric acid and stored for at least 24 h prior to the analysis of dissolved
181 iron. Dissolved iron was determined by flow injection analysis with colorimetric detection after
182 in-line pre-concentration on resin-immobilized 8-hydroxyquinoline (Sedwick et al., 2008).

183 2.2. Statistical analyses

184 Comparisons between data sets were made using analyses of variance. An *a priori* limit of
185 significance was set as $p < 0.05$. Data were tested for normality and homogeneity of variance,
186 and ANOVAs were performed using R (v2.13.2). Stations selected for a comparison of the
187 effects of assemblage composition were chosen based on HPLC analysis of pigments and the
188 contribution of each functional group to total chlorophyll (Mackey et al., 1996). When pigment
189 data were not included in the published reports, taxonomic discrimination was made by reported
190 microscopic results.

191

192 3. Results

193 3.1. IVARS, CORSACS and PRISM Photosynthesis/Irradiance Determinations

194 P-E determinations in IVARS were conducted during the peak of the spring bloom (generally
195 late December) and at the end of summer (early February) (Smith et al., 2011a). Ice
196 concentrations were $< 15\%$ at all stations. Average α^B , P_m^B and E_k values for the IVARS spring
197 and summer cruises were 0.040 ± 0.035 and $0.053 \pm 0.035 \mu\text{g C } (\mu\text{g chl})^{-1} \text{ h}^{-1}$ ($\mu\text{mol quanta m}^{-2}$
198 s^{-1})⁻¹, 1.3 ± 0.72 and $0.68 \pm 0.34 \mu\text{g C } (\mu\text{g chl})^{-1} \text{ h}^{-1}$, and 42 ± 29 and $23 \pm 30 \mu\text{mol quanta m}^{-2}$
199 s^{-1} , respectively (Table 2). P_m^B values of the two seasons were significantly different ($p < 0.05$),
200 but α^B and E_k values were not.

201 CORSACS measurements were largely conducted as part of experiments that manipulated
202 irradiance (7 and 33% of surface irradiance), iron concentrations (ambient and +1 nM), and CO₂

203 concentrations (380 and 750 μatm) (Feng et al., 2010). Natural populations were used as inocula
204 in semi-continuous cultures grown at constant irradiances (Hutchins et al., 2003), and P-E
205 determinations were made through time on all treatments to assess the impact of each variable
206 (and their interactions) on short-term photosynthetic responses. Irradiance variations resulted in
207 significantly ($p < 0.05$) decreased P_m^B and increased α^B values at the low and constant
208 irradiances used (Fig. 2). No net changes were noted in E_k means. Increased CO_2 concentrations
209 also resulted in significantly ($p < 0.05$) increased α^B and P_m^B values, although again little net
210 change was noted in E_k values. Finally, increased iron concentrations in these experiments did
211 not impact either α^B or P_m^B values significantly (Fig. 2). However, iron concentrations at the end
212 of the 18-day experiment ranged from 0.09 – 0.98 nM and were largely above concentrations
213 that are considered to be limiting (Timmermans et al., 2004). Therefore, any effect of iron on
214 photosynthetic parameters was not well tested in this experiment. Observed mean P_m^B values
215 were greater than those representing sub-optimal, in situ conditions such as in IVARS and
216 PRISM.

217 PRISM samples investigated the broad spatial patterns of P-E responses (Table 2). The mean
218 α^B and P_m^B values were 0.035 ± 0.020 ($\mu\text{g C} (\mu\text{g chl})^{-1} \text{h}^{-1} (\mu\text{mol quanta m}^{-2} \text{s}^{-1})^{-1}$) and 1.1 ± 0.50
219 $\mu\text{g C} (\mu\text{g chl})^{-1} \text{h}^{-1}$, respectively. The average E_k value was 52 ± 48 $\mu\text{mol quanta m}^{-2} \text{s}^{-1}$. There
220 was no significant difference between PRISM P-E parameters and those collected during IVARS
221 (December, February, or the total data set), and again no spatial pattern was observed.

222 Temperature, iron and nitrate concentrations were measured during PRISM at a number of
223 stations where P-E measurements were conducted (McGillicuddy et al., in press). The data were
224 arbitrarily divided above and below 20 $\mu\text{M NO}_3$ and above and below 0°C , and the P-E
225 parameters compared. Dissolved Fe concentrations ranged from 0.066 to 0.69 nM, and nitrate

226 ranged from 9.1 to 30.6 μM . Sample temperatures ranged from -1.6 to 2.6°C; 58 of the 102 P-E
227 determinations were below 0°C, and 44 were above. No significant difference in the mean α^B ,
228 P_m^B or E_k values were observed between the stations with nitrate concentrations less than 20 μM
229 and those with concentrations $> 20 \mu\text{M}$ (Table 3), which is not unexpected as these
230 concentrations are considered to be far above levels thought to be limiting. In contrast, at
231 stations with Fe concentrations below and above 0.10 nM (a level that approximates the onset of
232 Fe limitation in Antarctic phytoplankton; Timmermans et al., 2004), P_m^B values were
233 significantly ($p < 0.01$) greater (1.6 ± 0.55 vs. 0.95 ± 0.44) at lower iron concentrations (Table
234 3). α^B and E_k values, however, were not significantly different, suggesting that iron largely
235 impacts irradiance-saturated photosynthetic rates, which in turn are largely controlled by carbon
236 fixation processes. No significant differences were noted for any of the three photosynthetic
237 parameters within the temperature data subset, corroborating the PRISM results (Table 3). This
238 result suggests that photosynthetic responses are largely independent of temperature over short
239 time scales.

240 There was no significant relationship in the combined IVARS, JGOFS and PRISM data
241 between in any photosynthetic parameter from samples collected at 50 vs. 1% of surface
242 irradiance. This lack of correlation differs from the CORSACS results (Fig. 2), which were
243 conducted under constant irradiance using natural assemblages (but which changed appreciably
244 during the experiments). Available irradiances at the time of sampling do not necessarily reflect
245 the irradiance that influenced growth over times scales of days to weeks, which are unknown and
246 likely highly variable. This indicates that there is no substantial photoacclimation within water
247 columns of the Ross Sea, which in turn may suggest that the time needed for acclimation at these
248 temperatures is longer than the time scales of water column perturbation.

249 3.2. Comparison with Previous P-E Determinations

250 Because P-E determinations have been conducted during the past two decades with a similar
251 methodologies, we merged all data from the Ross Sea to assess the average photosynthetic
252 response by season (Table 4). There is a significant difference between austral spring and
253 summer averages for P_m^B and α^B values, with spring having a greater P_m^B (1.4 vs. 0.86) and α^B
254 values (0.034 vs. 0.023). However, no significant difference was observed between spring and
255 summer E_k values. Values of α^B and P_m^B were linearly correlated ($P_m^B = 10.9\alpha^B + 0.070$; $R^2 =$
256 0.15 ; $p < 0.001$; Fig. 3), as has been found previously (Harrison and Platt, 1980; van Hilst and
257 Smith, 2002; Behrenfeld et al., 2004), but the large amount of variability in the relationship
258 suggests that each is being influenced by multiple independent factors as well. No interannual
259 temporal trend was obvious, and interannual variability was substantial (Table 4). The overall
260 P_m^B average for all samples (N = 417) equaled $1.1 \pm 0.60 \mu\text{g C } (\mu\text{g chl})^{-1} \text{ h}^{-1}$, $\alpha^B = 0.030 \pm 0.023$
261 $\mu\text{g C } (\mu\text{g chl})^{-1} \text{ h}^{-1} (\mu\text{mol quanta m}^{-2} \text{ s}^{-1})^{-1}$ and $E_k = 44 \pm 27 \mu\text{mol quanta m}^{-2} \text{ s}^{-1}$.

262 3.3. Controls by Environmental Factors and Phytoplankton Composition

263 We tested for the effects of nitrate and temperature from the depth of sampling on P-E
264 parameters from all cruises. The data were arbitrarily divided above and below $20 \mu\text{M NO}_3$ and
265 above and below 0°C , and the P-E parameters compared. Nitrate concentrations at the time of
266 sampling ranged from $9.1 - 30.6 \mu\text{M}$, and 56 P-E measurements were conducted with NO_3
267 concentrations greater than $20 \mu\text{M}$. 58 analyses were conducted with NO_3 levels less than 20
268 μM . Sample temperatures ranged from $-1.6 - 2.6^\circ\text{C}$; 58 of the 102 P-E determinations were
269 below 0°C , and 44 were above. No significant differences were noted for any of the three
270 photosynthetic parameters within the nitrate or temperature data subsets, corroborating the

271 PRISM results (Table 3). This suggests that photosynthetic responses are largely independent of
272 these environmental controls over short time scales.

273 The two dominant functional groups in the Ross Sea, diatoms and haptophytes (largely
274 *Phaeocystis antarctica*), have different temporal and spatial distributions, with *P. antarctica*
275 generally dominating in spring in water columns with deeper vertical mixing, and diatoms
276 dominating in more stratified, summer conditions (Smith et al., 2014a). *P. antarctica* largely
277 occurs in cold waters ($< 0^{\circ}\text{C}$) and is responsible for the spring reduction in micro- and
278 macronutrients (Liu and Smith, 2012). To investigate if the two taxa have different
279 photosynthesis-irradiance responses, we selected 20 stations for each group that were identified
280 by chemical or microscopic means as being dominated by one of these groups, and assessed their
281 P-E characteristics (Table 5). We found no statistical difference between the two groups with
282 respect to α^B , P_m^B or E_k values.

283

284 **4. Discussion**

285 *4.1. Overall Patterns of Photosynthetic Parameters*

286 One major finding of this meta-analysis is that the average maximum, light-saturated rate of
287 photosynthesis equals $1.1 \mu\text{g C } (\mu\text{g chl})^{-1} \text{ h}^{-1}$ (Table 4). This is similar to the P_{opt}^B value
288 determined from Behrenfeld and Falkowski's (1997) polynomial equation ($1.3 \mu\text{g C } (\mu\text{g chl})^{-1}$
289 h^{-1}) at 0°C , despite the difference between P_{opt}^B and P_m^B as well as the range of temperatures at
290 which the P-E determinations were conducted. Our results reinforce the validity of using their
291 equation to estimate maximum photosynthetic rates and primary productivity within the waters
292 of the Ross Sea, and presumably the entire Southern Ocean. This average can also be used in
293 other bio-optical models of production to constrain the rates of carbon fixation over broad areas

294 (e.g., Arrigo et al., 2003, 2008). However, given the seasonal variability observed, more detailed
295 models that incorporate seasonal and environmental impacts on photosynthetic parameters may
296 require inclusion of other oceanographic variables (especially iron concentrations) to more
297 accurately predict production.

298 We found relatively minor spatial differences in photosynthetic parameters, but significant
299 seasonal differences. Specifically, α^B and P_m^B values of the entire meta-analysis data set were
300 significantly greater during spring than summer (both $p < 0.001$), which is consistent with the
301 large seasonal changes found in nearly all oceanographic and biological variables. The macro-
302 environment of the Ross Sea continental shelf changes markedly from spring to summer, with
303 increased temperatures, stronger vertical stratification, shallower mixed layers, decreased macro-
304 and micronutrient concentrations, and an altered assemblage composition (Smith et al., 2012).
305 All of these variables have been shown to influence P-E responses in laboratory and field studies
306 (e.g., MacIntyre et al., 2002; Xie et al., 2015), and as such, it is not surprising that the P-E
307 parameters also changed. It is tempting to suggest that the seasonal changes were driven by
308 changes in phytoplankton composition, but we believe that the seasonal changes in
309 oceanographic conditions led to in changes in P-E parameters as well as in composition, and that
310 both oceanographic changes and phytoplankton composition contributed to the seasonal
311 differences in P-E parameters we observed. An experiment which isolates natural assemblages
312 (perhaps a Lagrangian tracking of a parcel of water that is dominated by one taxa or a large-
313 volume mesocosm experiment such as has been conducted in the Baltic Sea; Riebesell et al.,
314 2013) would be more definitive test of the impacts of composition and the seasonal changes in P-
315 E parameters. Clearly the growth environment usually found in summer in the Ross Sea is not
316 favorable to high photosynthetic rates, a conclusion that have been consistently corroborated by

317 direct measurements of productivity (e.g., Long et al., 2011). It was impossible to accurately
318 assess interannual variations in P_E parameters, given the relatively low numbers of samples in
319 some years, but in view of the large variations observed in biomass and productivity from 1995
320 through 2010 (Smith and Comiso, 2008; Smith et al., 2011a), any interannual trend is likely
321 obscured by the substantial seasonal variability.

322 4.2. Controls of Photosynthesis-Irradiance Parameters

323 While not all data sets had complete macro- and micronutrient data available for inclusion,
324 we were unable to detect any controls of short-term photosynthetic rates by temperature or
325 nitrate within the seasonal data sets. The temperature range was modest (ca. 4°C), so the direct
326 impact of temperature may have been limited and obscured by other factors. Liu and Smith
327 (2012) demonstrated that the environmental factor that had the strongest impact on
328 phytoplankton biomass and composition was temperature. They found that that diatoms were
329 more likely to be found in waters above 0°C, and in sub-zero waters assemblage composition
330 was more often dominated by *Phaeocystis antarctica*. Waters with temperatures less than 0°C
331 also tend to have deeper mixed layers, reducing mean irradiance available for growth, which also
332 favors the growth of *P. antarctica* (Tremblay and Smith, 2007). Nitrate concentrations varied
333 more widely (from 9.3 to 31 µM), but still remained above those thought to limit nitrogen uptake
334 (Cochlan et al., 2002). Xie et al. (2015) also did not find a correlation between nutrients and
335 P_m^B , and suggested that this reflected the lag time between nutrient inputs and phytoplankton
336 growth in the English Chanel. They also found a complicated relationship between
337 photosynthetic parameters and temperature and suggested that each functional group had
338 temperature optima that were characterized by specific photosynthetic responses.

339 Reduced in situ iron concentrations in PRISM, however, resulted in elevated P_m^B values,
340 despite the relatively limited number of measurements at concentrations less than 0.1 nM (Table
341 3). In contrast, we did not detect a change at the end of the controlled experiments (CORSACS)
342 in which iron concentrations were measured. However, all but one of those conditions had
343 dissolved Fe concentrations > 0.13 nM (Feng et al., 2010) at the end of the 18-day experiment,
344 concentrations which are greater than those generally found in situ (Sedwick et al., 2011).
345 Furthermore, given that the lowest Fe concentration at the experiment's termination was 0.09
346 nM, it would be expected that preceding levels were even greater and may have obscured any Fe
347 effect. Because the experiments were completed in a constant irradiance environment, the
348 impact of iron also may have been lessened. Iron influences growth rates of Antarctic diatoms
349 (Timmermans et al., 2004), but growth rate responses are integrated over many days, whereas P-
350 E responses are not immediately influenced by iron additions (Hiscock et al., 2008). It is
351 tempting to suggest that the reduced summer P-E parameters may have resulted from iron
352 limitation, but iron availability is rarely determined in parallel with P-E parameters. We suggest
353 that the impacts of iron we observed – significantly increased P_m^B values under low Fe
354 concentrations – were mediated by a long-term assemblage response rather than an impact on
355 short-term photosynthetic rates. Iron limitation can impact chlorophyll synthesis (in a manner
356 similar to irradiance), and under iron and irradiance co-limitation, chlorophyll levels can be
357 elevated (Sunda and Huntsman, 1997), which would result in altered P_m^B values. Determination
358 of the exact cause of the iron effect on P_m^B , however, is impossible with the present data set.

359 The CORSACS experiments showed a clear impact of both irradiance and $[\text{CO}_2]$ on
360 photosynthetic responses. Under low and constant irradiance conditions (ca. 7% that of surface
361 irradiance), there was an increase in the light-limited rates of photosynthesis (α^B) and light-

362 saturated (P_m^B) values (Fig. 2). Low irradiance conditions often generate increased chlorophyll
363 concentrations per cell, but can also generate increased photosynthetic efficiencies (via changes
364 in photosynthetic units), which can result in elevation of both parameters (Prezelin, 1981;
365 Dubinsky and Stambler, 2009). P_m^B reflects the light-saturated rate, and presumably is set by the
366 amount of carbon that can be reduced by the cells, which in turn is thought to be limited by the
367 amount of chemical energy generated by the cells' photosystems. Increasing carbon dioxide
368 concentrations resulted in a marked and significant increase in P_m^B and α^B values, reinforcing the
369 classical view of the limitation of short-term photosynthesis by carbon availability under high
370 irradiance conditions. Enhanced α^B values may reflect the interaction between light-limited and
371 light-saturated rates described by Behrenfeld et al. (2004), in which the two co-vary and result in
372 the maintenance of a relatively constant E_k . Interestingly, increased CO₂ levels had little impact
373 on phytoplankton composition (Tortell et al., 2008b), and independent measurements suggest
374 that most Antarctic phytoplankton have a relatively broad capability to use a wide range of
375 carbon dioxide concentrations (Tortell et al., 2008a). Although it is tempting to suggest that
376 future increases in oceanic CO₂ concentrations might increase maximum photosynthetic rates,
377 such changes need to be assessed using long-term experiments that allow for acclimation and
378 adaptation over many generations (e.g., Lohbeck et al., 2012).

379 The influence of phytoplankton composition was insignificant (Table 5). This is consistent
380 with the previous results of van Hilst and Smith (2002) and Robinson et al. (2003) using a less
381 extensive data set, but in contrast to the extensive laboratory results of Arrigo et al. (2010), who
382 found that α^B and P_m^B values of *P. antarctica* grown at constant irradiances (from 5 – 125 μmol
383 quanta $\text{m}^{-2} \text{s}^{-1}$) and saturating nutrients were always greater than those of the diatom
384 *Fragilariopsis cylindrus*. The diatom had low P_m^B [from 0.46 to 0.54 $\mu\text{g C} (\mu\text{g chl})^{-1} \text{h}^{-1}$] and

385 α^B values [0.014 to 0.043 ($\mu\text{g C } (\mu\text{g chl})^{-1} \text{ h}^{-1} (\mu\text{mol quanta m}^{-2} \text{ s}^{-1})^{-1}$)] when compared to those
386 of the haptophyte (from 1.4 to 6.4, and 0.038 to 0.11, respectively). The diatom parameters
387 determined in culture were lower than in our data subset, and the haptophyte values higher; these
388 differences likely reflect the parameters of the individual species cultured and/or the acclimation
389 to constant culturing conditions. The in situ data also had substantial variability, which likely
390 resulted at least in part from the environmental conditions that allowed one particular functional
391 group to dominate. In addition to the influence of environmental conditions, individual species
392 likely have evolved mechanisms to permit adaptation within a wide environmental range.
393 Appearance of taxa in situ reflects a long-term process involving both growth and losses, and
394 both field and laboratory data suggest that the P-E parameters of the dominant forms in spring
395 and summer reflect the importance of selected environmental features (irradiance, iron) on their
396 long-term success within the water column.

397 In summary, the broad photosynthetic responses of Ross Sea phytoplankton are consistent
398 with the patterns used in global production estimates from satellite biomass estimates. However,
399 strong and significant seasonal differences occur, as do variations driven by irradiance, iron
400 concentrations, and carbon dioxide levels. Such significant differences may need to be included
401 in regional models of productivity and carbon flux. While these results may suggest that future
402 changes in photosynthetic capacity and production in the Ross Sea as a result of climate change
403 could be substantial, confirmation of this awaits future analyses of these parameters.

404

405 *Acknowledgements.* This research was supported by National Science Foundation grant ANT-
406 0944254 to WOS. P. Sedwick generously allowed the use of his iron data from the PRISM

407 cruise. We thank all our colleagues for their assistance at sea, especially L. Delizo and V. Asper.

408 This is VIMS contribution number XXXX.

409

410

411 **References**

- 412 Arrigo, K.R., Perovich, D.K., Pickart, R.S., Brown, Z.W., van Dijken, G.L., Lowry, K.E., Mills,
413 M.M., Palmer, M.A., Balch, W.M., Bahr, F., Bates, N.R., Benitez-Nelson, C., Bowler, B.,
414 Brownlee, E., Ehn, J.K., Frey, K.E., Garley, R., Laney, S.R., Lubelczyk, L., Mathis, J.,
415 Matsuoka, A., Mitchell, B.G., Moore, G.W.K., Ortega-Retuerta, E., Pal, S., Polashenski,
416 C.M., Reynolds, R.A., Scheiber, B., Sosik, H.M., Stephens, M., and Swift, J.H.: Massive
417 phytoplankton blooms under Arctic sea ice. *Science*, 336, 1408, 2013.
- 418 Arrigo, K.R., van Dijken, G.L., and Bushinsky, S.: Primary production in the Southern Ocean,
419 1997-2006. *J. Geophys. Res.*, 113, C08004, doi:10.1029/2007JC004551, 2008.
- 420 Arrigo, K.R., Worthen, D.L., and Robinson, D.H.: A coupled ocean-ecosystem model of the
421 Ross Sea: 2. Iron regulation of phytoplankton taxonomic variability and primary production.
422 *J. Geophys. Res.*, 108, doi:10.1029/2001JC000856, 2003.
- 423 Arrigo, K.R., Mills, M.M., Kropuenske, L.R., van Dijken, G.L., Alderkamp, A.-C., and
424 Robinson, D.H.: Photophysiology in two major Southern Ocean phytoplankton taxa:
425 photosynthesis and growth of *Phaeocystis antarctica* and *Fragilariopsis cylindrus* under
426 different irradiance levels. *Integr. Comp. Biol.*, 50, 950-966, 2010.
- 427 Behrenfeld, M.J. and Falkowski, P.G.: Photosynthetic rates derived from satellite-based
428 chlorophyll concentrations. *Limnol. Oceanogr.*, 42, 1-20, 1997.
- 429 Behrenfeld, M.J., Prasil, O., Babin, M., and Bruyant, F.: in search of a physiological basis for
430 covariations in light-limited and light-saturated photosynthesis. *J. Phycol.*, 40, 4-25, 2004.
- 431 Brightman, R.I. and Smith Jr., W.O.: Photosynthesis-irradiance relationships of Antarctic
432 phytoplankton during austral winter, *Mar. Ecol. Prog. Ser.*, 53, 143-151, 1989.
- 433 Brown, W. and Arrigo, K.R.: Contrasting trends in sea ice and primary production in the Bering
434 Sea and Arctic Ocean, *ICES. J. Mar. Sci.*, 69, 1180–1193, doi:10.1093/icesjms/fss113, 2012.

435 Cochlan, W.P., Bronk, D.A., and Coale, K.H.: Trace metals and nitrogenous nutrition of
436 Antarctic phytoplankton: experimental observations in the Ross Sea. *Deep-Sea Res. II*, 49,
437 3365-3390, 2002.

438 Denman, K.L. and Marra, J.: Modelling the time dependent photoadaptation of phytoplankton to
439 fluctuating light. In *Marine Interfaces Ecohydrodynamics*, edited by J.C. Nioul, Elsevier
440 Oceanography Series, 42, 341-359, 1986.

441 Dubinsky, Z. and Stambler, N.: Photoacclimation processes in phytoplankton: mechanisms,
442 consequences, and applications. *Aq. Micro. Ecol.*, 56, 163-176, 2009.

443 Feng, Y., Hare, C.E., Rose, J.M., Handy, S.M., DiTullio, G.R., Lee, P., Smith Jr., W.O.,
444 Peloquin, J., Tozzi, S., Sun, J., Zhang, Y., Dunbar, R.B., Long, M.C., Sohst, B., and
445 Hutchins, D.: Interactive effects of CO₂, irradiance and iron on Ross Sea phytoplankton.
446 *Deep-Sea Res. I*, 57, 368-383, doi:10.1016/j.dsr.2009.20.1013, 2009.

447 Harrison, W.G. and Platt, T.: Variations in assimilation number of coastal marine
448 phytoplankton: effects of environmental co-variates, *J. Plankton Res.*, 2, 249-260, 1980.

449 Hiscock, M.R.: The regulation of primary productivity in the Southern Ocean. PhD. Diss., Duke
450 Univ., 120 pp., 2004.

451 Hiscock, M.R., Lance, V.P., Apprill, A.M., Johnson, Z., Bidigare, R.R., Mitchell, B.G., Smith
452 Jr., W.O., and Barber, R.T.: Photosynthetic maximum quantum yield increases are an
453 essential component of Southern Ocean phytoplankton iron response. *Proc. Nat. Acad.*
454 *Sciences*, 105, 4775-4780, 2008.

455 Hutchins, D.A., Hare, C.E., Pustizzi, F.P, Trick, C.G., and DiTullio, G.R.: A shipboard natural
456 community continuous culture system to examine effects of low-level nutrient enrichments
457 on phytoplankton community composition. *Limnol. Oceanogr.-Methods*, 1, 82-91, 2003.

458 Huot, Y, Babin, M., and Bruyant, F.: Photosynthetic parameters in the Beaufort Sea in relation to
459 the phytoplankton community structure. *Biogeosci.*, 10, 3445-3454, 2013.

460 JGOFS: Protocols for the Joint Global Ocean Flux Study (JGOFS) core measurements. IOC
461 SCOR Rpt. 19, Bergen, Norway, 1996.

462 Kropuenske, L.R., Mills, M.M., Van Dijken, G.L., Bailey, S., Robinson, D.H., Welschmeyer,
463 N.A., and Arrigo, K.R.: Photophysiology in two major Southern Ocean phytoplankton taxa:
464 photoprotection in *Phaeocystis antarctica* and *Fragilariopsis cylindrus*. *Limnol. Oceanogr.-*
465 *Methods*, 54, 1176-1196, 2009.

466 Laws, E.A., DiTullio, G.R., Carder, K.L., Betzer, P.R., and Hawes, S.: Primary production in the
467 deep blue sea. *Deep-Sea Res.*, 37, 715-730, 1990.

468 Lewis, M.R. and Smith, J.C.: A small volume, short-incubation-time method for measurement of
469 photosynthesis as a function of incident irradiance. *Mar. Ecol. Prog. Ser.*, 13, 99-102, 1983.

470 Liu, X., and Smith Jr., W.O.: A statistical analysis of the controls on phytoplankton distribution
471 in the Ross Sea, Antarctica. *J. Mar. Systems*, 94, 135-144, 2012.

472 Lohbeck, K.T., Riebesell, U., and Reutsch, T.B.H.: Adaptive evolution of a key phytoplankton
473 species to ocean acidification. *Nature Geosci.*, 5, 346-351, 2012.

474 Long, M.C., Dunbar, R.B., Tortell, P.D., Smith Jr., W.O., Mucciarone, D.A., and DiTullio, G.R.:
475 Vertical structure, seasonal drawdown, and net community production in the Ross Sea,
476 Antarctica. *J. Geophys. Res.*, 116, C10029, doi:10.1029/2009JC005954, 2011.

477 MacIntyre, H.L, Kana, T.M., Anning, T., and Geider, R.J.: Photoacclimation of photosynthesis
478 irradiance response curves and photosynthetic pigments in microalgae and cyanobacteria. *J.*
479 *Phycol.*, 38, 17-38, 2002.

480 Mackey, M.D., Mackey, D.J., Higgins, H.W., and Wright, S.W.: CHEMTAX – a program for
481 estimating class abundances from chemical markers: application to HPLC measurements of
482 phytoplankton. *Mar. Ecol. Prog. Ser.*, 144, 265-283, 1996.

483 Marra, J., Heinemann, K., and Landriau, G. Jr.: Observed and predicted measurements of
484 photosynthesis in a phytoplankton culture exposed to natural irradiance. *Mar. Ecol. Prog.*
485 *Ser.*, 24, 43-50, 1985.

486 McGillicuddy, D.M. Jr., Sedwick, P.N., Dinniman, M.S., Arrigo, K.R., Bibby, T.S., Greenan,
487 B.J.W., Hofmann, E.E., Klinck, J.M., Smith Jr., W.O., Mack, S.L., Marsay, C.M., Sohst,
488 B.M., and G. van Dijken. 2015. Iron supply and demand in an Antarctic shelf system.
489 *Geophys. Res. Letters* (in press).

490 Moline, M.A., Schofield, O., and Boucher, N.P.: Photosynthetic parameters and empirical
491 modelling of primary production: a case study on the Antarctic Peninsula shelf. *Ant. Sci.*,
492 10, 45-54, 1998.

493 Montes-Hugo, M., Doney, S.C., Ducklow, H.W., Fraser, W., Martinson, D., Stammerjohn, S.E.,
494 and Schofield, O.: Recent changes in phytoplankton communities associated with rapid
495 regional climate change along the Western Antarctic Peninsula. *Science*, 323, 1470-3, 2008.

496 Peloquin, J. A. and Smith Jr., W.O.: Phytoplankton blooms in the Ross Sea, Antarctica:
497 Interannual variability in magnitude, temporal patterns, and composition. *J. Geophys. Res.*,
498 112, C08013, doi: 10.1029/2006JC003816, 2007.

499 Platt, T., Gallegos, C.L., and Harrison, W.G.: Photoinhibition of photosynthesis in natural
500 assemblages of marine phytoplankton. *J. Mar. Res.*, 38, 687-701, 1980a.

501 Platt, T., Harrison, W.G., Irwin, B., Horne, E.P., and Gallegos, C.L.: Photosynthesis and
502 photoadaptation of marine phytoplankton in the arctic. *Deep-Sea Res.*, 29, 1159-1170,
503 1980b.

504 Platt, T. Sathyendranath, S., and Fuentes-Yaco, C.: Biological oceanography and fisheries
505 management: perspective after 10 years. *ICES J. Mar. Sci.*, 5, 863-869, 2007.

506 Prezelin, B.B.: Light Reactions in Photosynthesis, in *Physiological Bases of Phytoplankton*
507 *Ecology*, edited by Platt, T., *Can. Bull. Fish. Aquat. Sci.* 210: 1-43, 1981.

508 Riebesell, U., Czerny, J., von Bröckel, K., Boxhammer, T., Büdenbender, J., Deckelnick, M.,
509 Fischer, M., Hoffmann, D., Krug, S.A., Lentz, U., Ludwig, A., Mucbe, R., and Schulz, K.G.:
510 Technical Note: A mobile sea-going mesocosm system – new opportunities for ocean change
511 research, *Biogeosci.*, 10, 1835-1847, 2013.

512 Robinson, D.H., Arrigo, K.R., DiTullio, G.R., and Lizotte, M.P.: Evaluating photosynthetic
513 carbon fixation during *Phaeocystis antarctica* blooms, in *Biogeochemistry of the Ross Sea*,
514 edited by DiTullio, G.R. and Dunbar, R.B., *Ant. Res. Ser.*, American Geophysical Union,
515 Washington, DC, 78, 77-92, 2003.

516 Rose, J.M., Feng, Y., DiTullio, G.R., Dunbar, R., Hare, C.E., Lee, P., Lohan, M., Long, M.,
517 Smith Jr., W.O., Sohst, B., Tozzi, S., Zhang, Y., and Hutchins, D.A.: Synergistic effects of
518 iron and temperature on Antarctic plankton assemblages. *Biogeosci.*, 6, 5,849-5,889, 2009.

519 Saggiomo, V., Catalano, G., Mangoni, O., Budillon, G., and Carrada, G.C.: Primary production
520 processes in ice-free waters of the Ross Sea (Antarctica) during the austral summer 1996.
521 *Deep-Sea Res. II*, 49, 1787-1801, 2002.

522 Sedwick, P.N., Bowie, A.R., and Trull, T.W.: Dissolved iron in the Australian sector of the
523 Southern Ocean (CLIVAR-SR3 section): meridional and seasonal trends. *Deep-Sea Res. I*,
524 55, 911–925, 2008.

525 Sedwick, P.N., Marsay, C.M., Aguilar-Islas, A.M., Lohan, M.C., Sohst, B.M., Long, M.C.,
526 Arrigo, K.R., Dunbar, R.B., Saito, M.A., Smith, W.O., and DiTullio, G.R.: Early-season
527 depletion of dissolved iron in the Ross Sea polynya: Implications for iron dynamics on the
528 Antarctic continental shelf. *J. Geophys. Res.*, 116, C12019, doi:10.1029/2010JC006553,
529 2011.

530 Smith Jr., W.O., Ainley, D.G., Arrigo, K.R., and Dinniman, M.S.: The oceanography and
531 ecology of the Ross Sea. *Annu. Rev. Mar. Sci.*, 6, 469-487, 2014a.

532 Smith Jr., W.O., Asper, V., Tozzi, S., Liu, X., and Stammerjohn, S.E.: Surface layer variability
533 in the Ross Sea, Antarctica as assessed by in situ fluorescence measurements. *Prog.*
534 *Oceanogr.*, 88, 28-45, 2011a.

535 Smith, W.O. Jr. and Comiso, J.C.: The influence of sea ice on primary production in the
536 Southern Ocean: a satellite perspective. *J. Geophys. Res.*, 113, C05S93,
537 doi:10.1029/2007JC004251, 2008.

538 Smith Jr., W.O., Dinniman, M.S., Hoffman, E.E., and Klinck, J.: Modeled impacts of changing
539 winds and temperatures on the oceanography of the Ross Sea in the 21st century. *Geophys.*
540 *Res. Letters* 41, doi:10.1002/2014GL059311, 2014b.

541 Smith Jr., W.O. and Jones, R.M.: Vertical mixing, critical depths, and phytoplankton growth in
542 the Ross Sea. *ICES J. Mar. Science*, doi:10.1093/icesjms/fsu234, 2014.

543 Smith Jr., W.O., Sedwick, P.N., Arrigo, K.R., Ainley, D.G., and Orsi, A.H.: The Ross Sea in a
544 sea of change. *Oceanogr.*, 25, 44-57, 2012.

545 Smith Jr., W.O., Shields, A.R., Dreyer, J., Peloquin, J.A., and Asper, V.: Interannual variability
546 in vertical export in the Ross Sea: magnitude, composition, and environmental correlates.
547 *Deep-Sea Res. I*, 58:,147-159, 2011b.

548 Smith Jr., W.O., Tozzi, S., Sedwick, P.W., DiTullio, G.R., Peloquin, J.A., Long, M., Dunbar, R.,
549 Hutchins, D.A., and Kolber, Z.: Spatial and temporal variations in variable fluorescence in
550 the Ross Sea (Antarctica): environmental and biological correlates. *Deep-Sea Res. I*, 79,
551 141-155, 2013.

552 Smyth, R.L., Sobrino, C., Phillips-Kress, J., Kim, H.-C., and Neele, P.J.: Phytoplankton
553 photosynthetic response to solar ultraviolet irradiance in the Ross Sea polynya: development
554 and evaluation of time-dependent model with limited repair. *Limnol. Oceanogr.*, 57, 1602-
555 1618, 2012.

556 Sunda, W.G. and Huntsman, S.A.: Interrelated influence of iron, light and cell size on marine
557 phytoplankton growth. *Nature* 390, 389–392, 1997.

558 Thompson, R.E. and Fine, I.V.: Estimating mixed layer depth from oceanic profile data. *J.*
559 *Atmos. Ocean. Tech.*, 20, 319–329, 2003.

560 Tilzer, M.M., Elbrachter, M., Gieskes, W.W., and Beese, B.: Light-temperature interaction in the
561 control of photosynthesis in Antarctic phytoplankton. *Polar Biol.*, 5, 105-111, 1986.

562 Timmermans, K.R., Gerringa, L.J.A., de Baar, H.J.W., van der Wagt, B., Veldhuis, M.J.W., de
563 Jong, J.T.M., Croot, P.L., and Boye, M.: Growth rates of large and small Southern Ocean
564 diatoms in relation to availability of iron in natural seawater. *Limnol. Oceanogr.*, 46, 260-
565 266, 2004.

566 Tortell, P.D., Payne, C., Gueguen, C., Strzepek, R.F., Boyd, P.W., and Rost, B.: Inorganic
567 carbon uptake by Southern Ocean phytoplankton. *Limnol. Oceanogr.*, 53, 1266-1278, 2008a.

568 Tortell, P.D., Payne, C., Li, Y., Trimborne, S., Rost, B., Smith Jr., W.O., Riesselman, C.,
569 Dunbar, R.B., Sedwick, P., and DiTullio, G.R.: CO₂ sensitivity of Southern Ocean
570 phytoplankton. *Geophys. Res. Letters*, 35, L04605, doi:10.1029/2007GL032583, 2008b.

571 Tremblay, J.-E., and Smith Jr., W.O.: Phytoplankton processes in polynyas, in *Polynyas:
572 Windows to the World's Oceans*, edited by Smith Jr., W.O. and Barber, D.G., Elsevier,
573 Amsterdam, 239-270, 2007.

574 van Hilst, C.M. and Smith Jr., W.O.: Photosynthesis/irradiance relationships in the Ross Sea,
575 Antarctica, and their control by phytoplankton assemblage composition and environmental
576 factors. *Mar. Ecol. Prog. Ser.*, 226, 1-12, 2002.

577 Xie, Y., Tilstone, G.H., Widdicombe, C., Woodward, E.M.S., Harris, C., and Barnes, M.K.:
578 Effect of increases in temperature and nutrients on phytoplankton community structure and
579 photosynthesis in the western English Channel. . *Mar. Ecol. Prog. Ser.*, 519, 61-73, 2015.

580

581 **Figure Legends**

582

583 Figure 1. Map showing the location of the stations where photosynthesis-irradiance
584 determinations were conducted.

585 Figure 2. Photosynthesis-irradiance parameters determined from experimental manipulations of
586 natural populations. Samples had either high or low (33 or 7% of surface value)
587 irradiance, high or low (750 or 380 ppm) CO₂, and high or low (+1 nM and ambient; ca.
588 0.1 nM) iron concentrations. Asterisks indicate a significant difference between the
589 high and low treatments within each variable (*: p < 0.05; **: p < 0.01; ***: p < 0.001).

590 Figure 3. Relationship of α^B (light-limited photosynthesis) and P_m^B (irradiance-saturated
591 photosynthesis) in samples from the Ross Sea. Solid line is the linear regression ($P_m^B =$
592 $10.9\alpha^B + 0.70$; $r^2 = 0.15$; $p < 0.001$).

593

594 Table 1. Listing of photosynthesis-irradiance responses used in this meta-analysis. N = number
 595 of determinations; V_{inc} = volume incubated; F/NF = filtered/not filtered.

Cruise Name	Dates of Sampling	N	V_{inc} (mL)	F/NF	Reference
RSP ²	11/16/1994 – 11/30/1995;	10	2	NF	van Hilst and Smith (2002)
	12/21/1995 – 1/13/1996	54	2	NF	
JGOFS	11/16/1996 – 12/11/2006	70	10	F	Hiscock (2004)
	1/12/1997 – 2/8/2007	87	10	F	
	4/17/2007 – 4/26/2007	5	10	F	
ROSSMIZ	1/11/1996 – 2/10/1996	72	50	F	Saggiomo et al. (2002)
ROAVERRS	11/10/1998 – 12/10/1998	15	2	F*	Robinson et al. (2003)
NBP05-08	11/8/2005 – 11/30/2005	10	5	NF	Smyth et al. (2012)
IVARS 1	12/19/2001 – 2/2/2002	6	2	NF	This report
IVARS 3	12/26/2003 – 2/6/2004	9	2	NF	This report
IVARS 4	12/19/2004 – 1/31/2005	16	2	NF	This report
IVARS 5	12/26/2005 – 1/2/2006	7	2	NF	This report
CORSACS 1	12/27/2005 – 1/31/2006	83	2	NF	This report
CORSACS 2	11/16/2006 – 12/11/2006	23	2	NF	This report
PRISM	1/8/2012 – 2/2/2012	77	2	NF	This report

596 *: Gravity filtration

597 Table 2. Mean and standard deviations of photosynthesis-irradiance parameters, mixed layer
598 depths (Z_{mix}) and euphotic zone depths ($Z_{1\%}$) determined during IVARS and PRISM cruises.
599 Units: α^B : $\mu\text{g C } (\mu\text{g chl})^{-1} \text{ h}^{-1}$ ($\mu\text{mol quanta m}^{-2} \text{ s}^{-1}$) $^{-1}$; P_m^B : $\mu\text{g C } (\mu\text{g chl})^{-1} \text{ h}^{-1}$; E_k : $\mu\text{mol quanta}$
600 $\text{m}^{-2} \text{ s}^{-1}$; Z_{mix} : m; $Z_{1\%}$: m. Number of observations in parentheses.

Month	Year	α^B	P_m^B	E_k	Z_{mix}	$Z_{1\%}$
December	2001	$0.060 \pm$	$2.3 \pm$	$42 \pm$	37 ± 13	$9.38 \pm$
		0.015 (4)	0.61	18	(17)	1.06 (8)
February	2002	0.008 (1)	0.85	110	35 ± 9	$14.3 \pm$
					(16)	2.74 (9)
December	2002	$0.033 \pm$	$0.97 \pm$	$34 \pm$	29 ± 7	$36.0 \pm$
		0.012 (4)	0.32	24	(8)	14.5 (3)
December	2003	$0.019 \pm$	$0.61 \pm$	$37 \pm$	23 ± 10	$27.8 \pm$
		0.005 (5)	0.36	28	(12)	11.4 (9)
February	2004	$0.067 \pm$	$0.80 \pm$	$16 \pm$	25 ± 9	$25.8 \pm$
		0.047 (4)	0.57	15	(25)	6.57 (12)
December	2004	$0.022 \pm$	$1.1 \pm$	$62 \pm$	21 ± 6	$23.8 \pm$
		0.009 (10)	0.42	38	(23)	7.66 (23)
February	2005	$0.051 \pm$	$0.57 \pm$	$14 \pm$	20 ± 7	$24.6 \pm$
		0.023 (6)	0.048	6.1	(24)	8.20 (25)
December	2005	$0.070 \pm$	$1.6 \pm$	$28 \pm$	20 ± 11	$24.0 \pm$
		0.055 (7)	0.80	11	(12)	1.91 (7)
Mean:	---	$0.040 \pm$	$1.3 \pm$	$42 \pm$	26 ± 12	$23.0 \pm$
December		0.035 (27)	0.72	29	(72)	10.1 (50)
Mean:	---	$0.053 \pm$	$0.68 \pm$	$23 \pm$	26 ± 10	$22.9 \pm$
February		0.035 (11)	0.34	30	(65)	8.13 (45)
PRISM,	2010	$0.035 \pm$	$1.1 \pm$	$52 \pm$	28 ± 23	42.2 ± 22.8
January		0.020 (77)	0.50	48	(116)	(116)

601

602 Table 3. Comparison of PRISM photosynthetic parameters as a function of nitrate, temperature
603 and iron (means and standard deviations). Range of data listed in parentheses. The available data
604 were divided into those stations that had nitrate concentrations above and below 20 μM , in situ
605 temperatures above and below 0°C , and iron concentrations greater than or less than 0.1 nM. No
606 significant differences were noted between the two sets of parameters except where noted.

Variable Group	N	α^B ($\mu\text{g C } (\mu\text{g chl})^{-1} \text{ h}^{-1}$ ($\mu\text{mol quanta m}^{-2} \text{ s}^{-1})^{-1}$)	P_m^B ($\mu\text{g C } (\mu\text{g chl})^{-1}$ h^{-1})	E_k ($\mu\text{mol quanta}$ $\text{m}^{-2} \text{ s}^{-1}$)
[NO ₃] < 20 μM	58	0.035 \pm 0.020 (0.012 – 0.095)	1.2 \pm 0.64 (0.29 – 3.1)	43 \pm 34 (7 – 193)
[NO ₃] > 20 μM	56	0.043 \pm 0.039 (0.008 – 0.183)	1.2 \pm 0.58 (0.21 – 2.8)	48 \pm 47 (4 – 238)
T > 0°C	44	0.040 \pm 0.036 (0.015 – 0.183)	1.2 \pm 0.66 (0.29 – 3.1)	44 \pm 40 (7 – 193)
T < 0°C	58	0.032 \pm 0.021 (0.011 – 0.095)	1.2 \pm 0.53 (0.21 – 2.7)	50 \pm 44 (8 – 238)
[Fe] < 0.1 nM	6	0.038 \pm 0.023 (0.021 – 0.053)	1.6 \pm 0.55** (1.1 – 2.7)	41 \pm 18 (28 – 54)
[Fe] > 0.1 nM	33	0.029 \pm 0.017 (0.011 – 0.066)	0.95 \pm 0.44 (0.21 – 1.7)	48 \pm 36 (8 – 131)

607 **: t-test indicated a significant difference ($p < 0.01$)

608

609 Table 4. Seasonal comparison of photosynthetic parameters from the Ross Sea.

Season	P_m^B ($\mu\text{g C } (\mu\text{g chl})^{-1} \text{ h}^{-1}$)	α^B ($\mu\text{g C } (\mu\text{g chl})^{-1} \text{ h}^{-1}$) ($\mu\text{mol quanta m}^{-2} \text{ s}^{-1}$) ⁻¹)	E_k ($\mu\text{mol quanta m}^{-2} \text{ s}^{-1}$)	N	Reference
Spring	1.7 ± 0.97	0.047 ± 0.023	37 ± 7.5	37	van Hilst and Smith (2002)
Summer	2.5 ± 1.3	0.087 ± 0.043	31 ± 16	31	
Spring	1.2 ± 0.54	0.036 ± 0.015	37 ± 13	70	Hiscock (2004)
Summer	0.64 ± 0.26	0.016 ± 0.007	44 ± 18	98	
Autumn	0.70 ± 0.13	0.040 ± 0.017	21 ± 9	5	
Summer	1.3 ± 0.39	0.073 ± 0.088	23 ± 8	51	Saggiomo et al. (2002)
Spring	1.8 ± 0.68	0.020 ± 0.004	89 ± 23	15	Robinson et al. (2003)
Spring ²	2.1 ± 0.48	0.072 ± 0.027	31 ± 8.0	10	Smyth et al. (2012)
Spring	1.3 ± 0.72	0.040 ± 0.035	42 ± 29	27	IVARS: This report
Summer	0.68 ± 0.34	0.053 ± 0.035	23 ± 30	11	IVARS: This report
Summer	1.1 ± 0.500	0.035 ± 0.020	52 ± 48	77	PRISM: This report
Mean Spring ¹	1.4 ± 0.63	0.034 ± 0.024	44 ± 25	159	---
Mean Summer ¹	0.86 ± 0.45	0.023 ± 0.018	43 ± 28	268	---
Overall Mean ¹	1.1 ± 0.60	0.030 ± 0.023	44 ± 27	417	---

610 ¹: Weighted mean of all samples

611 ²: α^B and E_k values calculated from data using factor described in original paper

612 Table 5. Comparison of the mean photosynthesis-irradiance parameters as a function of
 613 phytoplankton composition (means and standard deviations). Dominance was determined by
 614 either chemical or microscopic analyses. Twenty stations for each functional group (N) from the
 615 entire data set were selected for inclusion in this comparison. No significant difference in any
 616 photosynthetic parameter was detected.

617

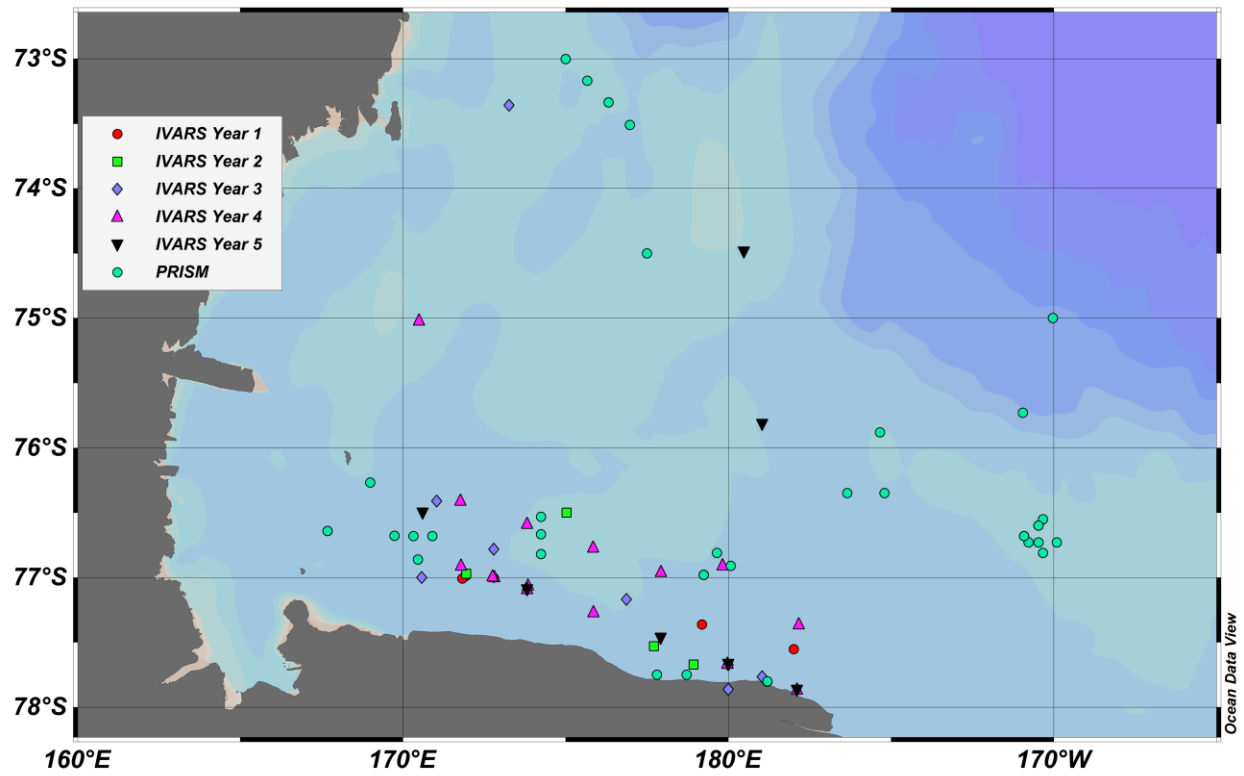
Functional Group	P_m^B ($\mu\text{g C } (\mu\text{g chl})^{-1} \text{ h}^{-1}$)	α^B ($\mu\text{g C } (\mu\text{g chl})^{-1} \text{ h}^{-1}$) ($\mu\text{mol quanta m}^{-2} \text{ s}^{-1}$) ⁻¹)	E_k ($\mu\text{mol quanta m}^{-2} \text{ s}^{-1}$)
<i>Phaeocystis</i> <i>antarctica</i> (N=20)	1.4 ± 0.76	0.067 ± 0.060	33 ± 23
Diatoms (N=20)	1.1 ± 0.63	0.050 ± 0.045	32 ± 19

618

619

620

621 Fig. 1.

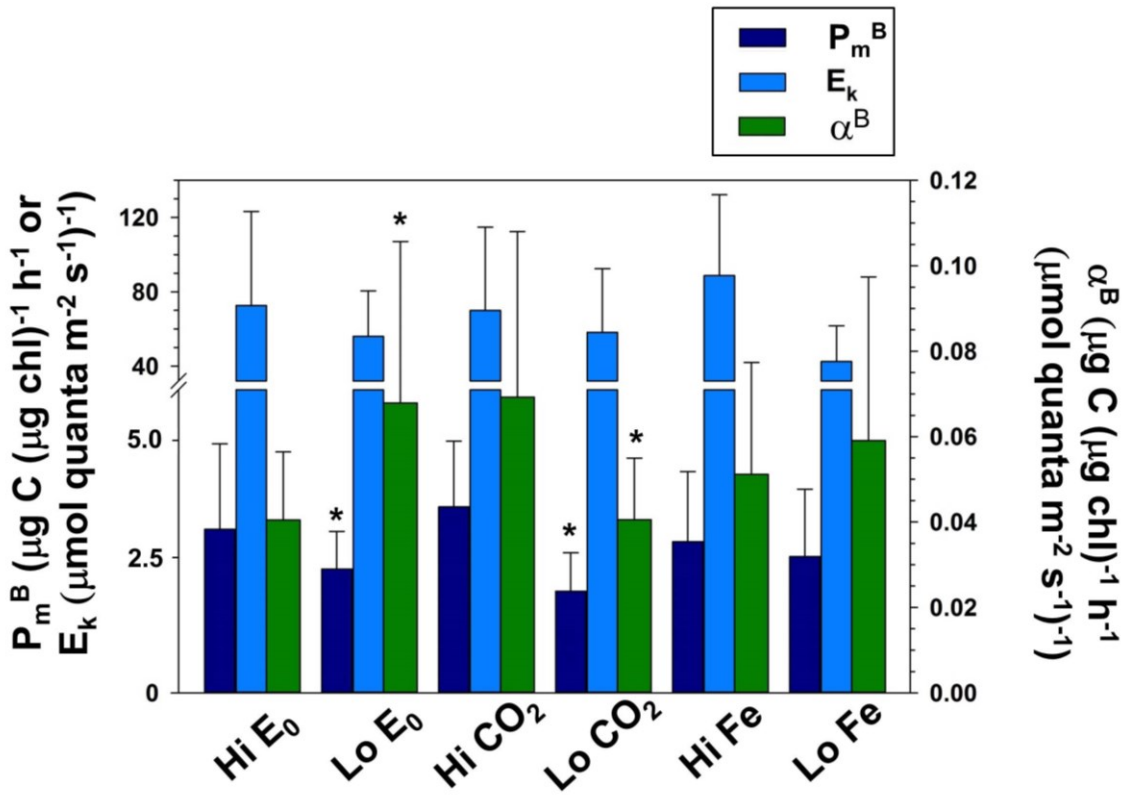


622

623

624

625 Fig. 2

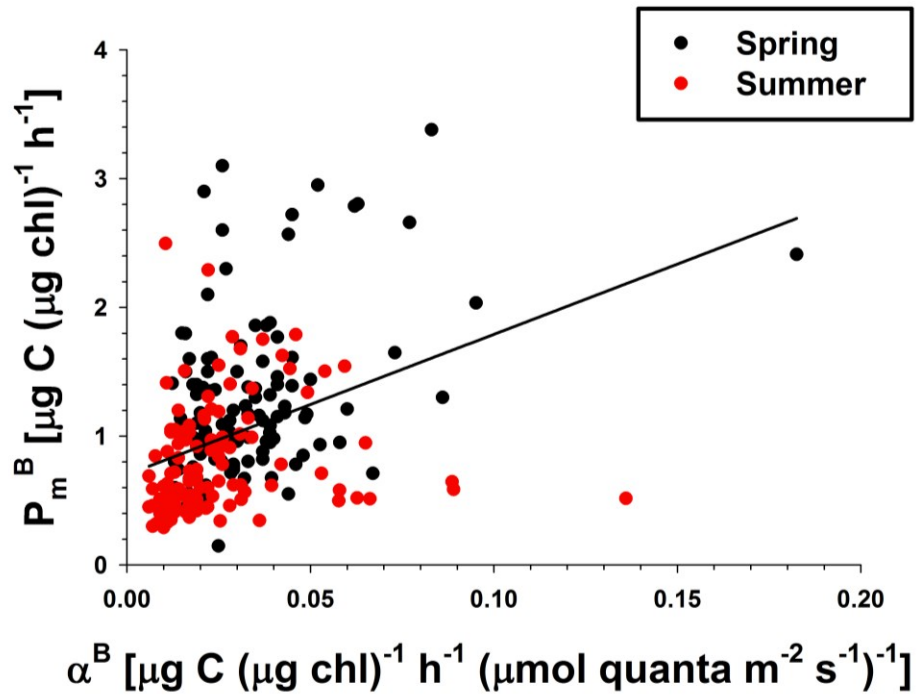


626

627

628 Figure 3.

629



630

631